

Study of Platinum Dissolution Mechanism Using a Highly Sensitive Electrochemical Quartz Crystal Microbalance

Takara Sakurai,¹ Masayo Shibata,¹ Reiko Horiuchi,¹ Ichizo Yagi,² and Toshihiro Kondo*¹

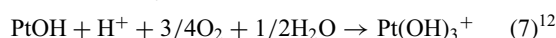
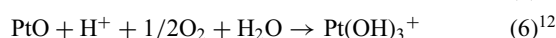
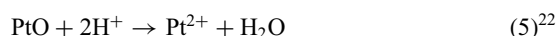
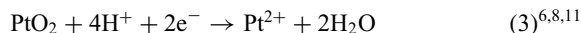
¹Graduate School of Humanities and Sciences, Ochanomizu University, 2-1-1 Ohtsuka, Bunkyo-ku, Tokyo 112-8610

²Fuel Cell Cutting-Edge Center Technology Research Association (FC-Cubic TRA), 2-3-36 Aomi, Koto-ku, Tokyo 135-0064

(Received December 1, 2010; CL-101015; E-mail: kondo.toshihiro@ocha.ac.jp)

Platinum (Pt) dissolution during oxidation/reduction cycle in various potential cycle ranges and in various pHs of the oxygen-saturated and deaerated H₂SO₄ and HClO₄ electrolyte solutions was monitored by the highly sensitive electrochemical quartz crystal microbalance (EQCM) system. It was found that the Pt mass reduction depended on the potential cycle range and pH of the electrolyte solution with dissolved oxygen. Based on these results, it can be suggested that the dissolution of Pt requires one proton per one Pt and that it also requires dissolved oxygen, and then we can conclude that the dissolution reaction of Pt is as follows; PtO + H⁺ + 1/2O₂ + H₂O → Pt(OH)₃⁺ and/or PtOH + H⁺ + 3/4O₂ + 1/2H₂O → Pt(OH)₃⁺.

It is well-known that Pt is one of the best cathodic catalysts for polymer electrolyte fuel cells (PEFC), which are expected to be a most attractive energy conversion device in the near future. Oxygen reduction reaction (ORR), namely, cathodic reaction in PEFC has been extensively studied by many groups.^{1,2} Since in PEFC, a serious problem is dissolution of Pt into electrolyte solution (or polymer electrolyte) during operation, for practical use, the durability of the electrode is an issue of concern. For solving this problem, the dissolution behavior should be monitored at an atomic level, and then the mechanism of dissolution should be clarified. Many research groups have investigated the dissolution of Pt with single crystal Pt,²⁻⁴ polycrystalline Pt,⁵⁻¹¹ Pt-nanoparticle-modified carbon,¹²⁻¹⁷ and Pt alloy^{2,18-21} electrodes using several analytical methods such as conventional electrochemical measurements,^{10,16} theoretical calculation,²² direct mass measurements,^{6,8} spectroscopic analyses,^{7,10d} ICP-MS,^{3,7a} XRD,^{7a,14,17,20,21} TEM,^{14,15,17,20} SEM,¹⁹ STM,⁵ AFM,^{7a,19} EDX,¹⁵ XPS,²⁰ XAS,¹³ and electrochemical quartz crystal microbalance (EQCM) measurements.^{7,11,18} However, microscopic, spectroscopic, and direct mass measurements cannot show the precise amounts of dissolved Pt because the amount of Pt dissolution is too small. Moreover, many intermediates were reported to be generated during PEFC operation. Several things reported previously were i) the origin of the dissolution of Pt is assumed to be Pt oxides,¹⁰ ii) Pt dissolution requires potential cycling,^{6,7a,9} iii) some impurities, such as SO₂, NO₂, and Cl⁻, contained in the electrolyte solutions accelerated the Pt dissolution,^{7,15,18} and iv) smaller Pt particles grew to be larger particles according to Ostwald ripening during potential cycling.^{5,13,14,21} However, it has not made clear this problem yet. We can assume that PEFC does not ideally contain any impurities, and the following reactions have been previously proposed as Pt dissolution reactions;



When the Pt dissolution takes place with the Pt oxidation at the same time, we cannot measure charge only due to the Pt dissolution. Thus, the quantitative relationship between amounts of dissolved Pt, concentration of H⁺, and dissolved oxygen should indicate which reaction is the true Pt dissolution reaction.

In order to make clear the reaction mechanism of Pt dissolution during potential cycling, in this study, we monitored the dissolution behavior of Pt during continuous potential cycling in various potential cycle ranges and in various pHs of the oxygen-saturated and deaerated H₂SO₄ and HClO₄ electrolyte solutions by highly sensitive EQCM. It was found that the Pt mass reduction depended on the potential cycle range and pH of the electrolyte solution with dissolved oxygen, suggesting that dissolution of Pt requires one proton per one Pt and also dissolved oxygen, and we conclude that the dissolution reaction is the above eqs 6 and/or 7.

A Au-coated QCM electrode, Pt wire, and MSE were used as working, counter, and reference electrodes, respectively. The potential values were referred to RHE. A Pt QCM electrode was prepared by electrochemical deposition in 0.1 M HClO₄ electrolyte solution containing 0.5 mM H₂PtCl₆ on the Au QCM electrode by previously reported procedures.⁷ The resonant frequency of the QCM electrodes, which was oscillated by an oscillation circuit, was monitored simultaneously with electrode potential and current by a frequency counter (QCM934, Seiko EG&G). The frequency stability of the present EQCM system was better than 0.1 Hz for a sampling gate time of 0.1 s. The mass sensitivity of the 27 MHz AT-cut quartz crystal used in the present study was ca. 0.271 ng Hz⁻¹. The calibration constant was determined by Cu deposition²³ using Sauerbrey's equation.²⁴ Mass change of Pt electrode during the potential cycling in the various potential ranges with a scan rate of 100 mV s⁻¹ was measured in oxygen-saturated or deaerated H₂SO₄ and HClO₄ electrolyte solutions under oxygen or nitrogen atmosphere, respectively. Values of pH were determined by a pH meter (S20, SevenEasy). All the measurements in this study were performed at 25 ± 0.05 °C, which was controlled by a thermostatic chamber (ESPEC Co., LU-113).

Figure 1 shows cyclic voltammograms (CVs) and potential dependence of mass change of the Pt QCM electrodes measured in (a) deaerated and (b) oxygen-saturated 0.050 M H₂SO₄. The oxidation/reduction current between +0.75 (vs. RHE) and +1.00 V is due to the surface oxidation/reduction of Pt. An

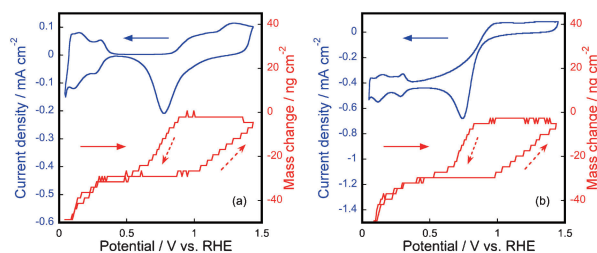


Figure 1. Potential dependence of current density and mass change of Pt QCM electrodes measured in (a) deaerated and (b) oxygen-saturated 0.050 M H₂SO₄ (pH 1.18) with a scan rate of 100 mV s⁻¹.

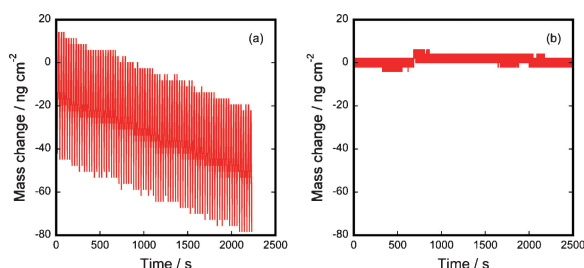


Figure 2. Time dependence of mass change measured in oxygen-saturated 0.50 M H₂SO₄ (pH 0.32) (a) when the potential was cycled between +0.05 and +1.45 V for 90 cycles and (b) when the potential was kept at +1.20 V for 2500 s.

oxidation/reduction couple current, attributed to hydrogen adsorption and desorption, was observed around +0.20 V. Real Pt area was calculated from the charge of hydrogen adsorption. In the relatively negative potential region, larger cathodic current was observed in the oxygen-saturated electrolyte solution, showing that the ORR took place in this potential region. The absolute value of mass change during one potential cycle was ca. 50 ng cm⁻² in both cases, and the shape of the mass change in the both cases was in good agreement with those reported previously.^{7,18} Then we can conclude that the observed mass change corresponds to the adsorption/desorption of water and sulfate anion onto/from the Pt surface, respectively, and surface oxide formation/reduction. These results show that the dissolved oxygen does not greatly affect water and/or sulfate adsorption/desorption.

Figure 2a shows time dependence of mass change of a Pt QCM electrode when the potential was cycled in oxygen-saturated 0.50 M H₂SO₄ (pH 0.32) with a scan rate of 100 mV s⁻¹ in the potential range between +0.05 and +1.45 V. Although mass change due to the Pt dissolution cannot be detected in one potential cycle (Figure 1), the gradual mass decrease can be clearly observed in this figure. The mass change due to Pt dissolution was calculated to be ca. 0.75 ng cm⁻² cycle⁻¹ from the slope. When the potential was kept for a longer time at +1.20 V, where Pt oxide (PtO₂) formed on the surface, no mass change was observed (Figure 2b), indicating that the Pt dissolution requires potential cycling. This result is supported by previous studies.^{6,7,9}

In order to make clear which potential range affects the dissolution, we measured the Pt dissolution when the negative and positive potential limits of the potential cycle changed in the

Table 1. Dependence of potential cycle range on the amount of Pt dissolution measured in oxygen-saturated 0.50 M H₂SO₄ (pH 0.32) with a scan rate of 100 mV s⁻¹

Negative potential limit/V	Positive potential limit/V	Mass change /ng cm ⁻² cycle ⁻¹
+0.60	+1.20	-0.75
+0.60	+1.15	-0.63
+0.60	+1.10	-0.32
+0.60	+1.00	0
+0.60	+0.90	0
+0.90	+1.20	0
+0.80	+1.20	-0.18

oxygen-saturated 0.50 M H₂SO₄ (pH 0.32). The obtained values are listed in Table 1. When the negative and positive potential limits were +0.60 and +1.20 V, respectively, the mass change was the same as that of potential cycling between +0.05 and +1.45 V, 0.75 ng cm⁻² cycle⁻¹. When the negative and positive potential limits were between +0.60 and +1.20 V, Pt was dissolved at less than 0.75 ng cm⁻² cycle⁻¹. When the negative potential limit was fixed to +0.60 V and the positive potential limit was +0.90 and +1.00 V, where the anodic current due to the surface oxide formation started to flow, Pt was not dissolved. When the positive potential was more than +1.10 V, where the surface seemed to be completely oxidized to PtO₂, the more positive potential limit was, the more Pt was dissolved until the positive potential limit was +1.20 V. When Pt was electrochemically oxidized, the surface species changed from Pt to PtOH, PtO, and then PtO₂. This suggests that the origin of the Pt dissolution was PtO and/or PtOH. When the positive potential limit was fixed at +1.20 V and the negative potential limit was +0.90 V, where the cathodic current due to the reduction of the surface oxide just started to flow, Pt was not dissolved. When the negative potential limit was +0.80 V, where a relatively small cathodic current was observed, Pt was a little dissolved. This suggests that when the surface oxide (PtO₂) was electrochemically reduced to PtO and/or PtOH and PtO/PtOH formed on the surface, Pt started to dissolve, indicating that the origin of the Pt dissolution should be PtO and/or PtOH. PtO and PtOH are intermediates during the surface oxide formation/reduction; their lifetime should be short and the PtO₂ formation is so fast that the amount of dissolution should be very small during one potential cycle.

Time dependence of mass change during 90 potential cycles was measured in oxygen-saturated H₂SO₄ and HClO₄ electrolyte solutions with various pHs. Dissolution of Pt was observed in every electrolyte solution during the potential cycling. These values were consistent with literature values,^{8a,18} meaning that even the small values observed in the present study should be reliable. The greater the pH of the electrolyte solution was, the less Pt was dissolved. The dissolved Pt was plotted as a function of the pH of the electrolyte solution in Figure 3. It is noted that the vertical axis in Figure 3 is a logarithm value of the concentration of dissolved Pt solution per one potential cycle. As clearly seen in Figure 3, a linear relationship with a slope of ca. -1 was observed, indicating that the reaction requires 1 proton per 1 Pt.

At the same pH, Pt dissolved more in H₂SO₄ than in HClO₄, outside the experimental error bar range. Sulfate anion is

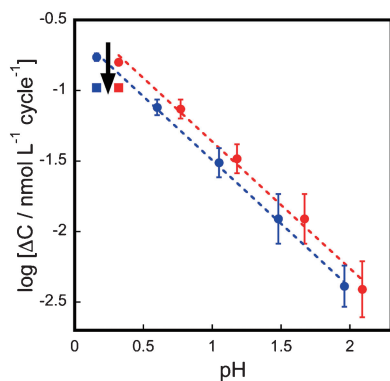


Figure 3. Amounts of Pt dissolution as a function of pH with a scan rate of 100 mV s^{-1} . Red and blue circles present the data measured in oxygen-saturated H_2SO_4 and HClO_4 , respectively. Red and blue squares present the data measured in deaerated H_2SO_4 and HClO_4 , respectively. Potential range is between $+0.05$ and $+1.45 \text{ V}$.

strongly adsorbed on the Pt surface more than perchlorate anion. Maybe the adsorbed sulfate anion accelerates the Pt surface oxidation or the adsorbed sulfate anion stabilizes the intermediates (PtO and/or PtOH) of the surface oxide formation (PtO_2), and then the Pt dissolution should be accelerated.

Based on the above results, the reaction of the Pt dissolution is as follows: $\text{PtO} + \text{H}^+ + 1/2\text{O}_2 + \text{H}_2\text{O} \rightarrow \text{Pt}(\text{OH})_3^+$ and/or $\text{PtOH} + \text{H}^+ + 3/4\text{O}_2 + 1/2\text{H}_2\text{O} \rightarrow \text{Pt}(\text{OH})_3^+$.

If the reaction of eqs 6 and/or 7 take place, the Pt dissolution requires not only protons but also dissolved oxygen. In order to confirm the effect of the dissolved oxygen on the Pt dissolution, the Pt dissolution behavior was monitored in $0.50 \text{ M H}_2\text{SO}_4$ and 1.0 M HClO_4 solutions deaerated by bubbling with pure N_2 (99.95%). As expected, when the Pt dissolution was measured in deaerated solutions, the amount of Pt dissolution decreased as closed squares shown in Figure 3. Even during the potential cycling, pure N_2 is flowing in the QCM cell but dissolved oxygen cannot be completely removed; a little Pt dissolution was observed. Thus, we can conclude that the Pt dissolution reaction is the chemical reaction of $\text{PtO} + \text{H}^+ + 1/2\text{O}_2 + \text{H}_2\text{O} \rightarrow \text{Pt}(\text{OH})_3^+$ and/or $\text{PtOH} + \text{H}^+ + 3/4\text{O}_2 + 1/2\text{H}_2\text{O} \rightarrow \text{Pt}(\text{OH})_3^+$.

Inzelt et al. investigated the dissolution of Pt with smooth and roughened Pt in H_2SO_4 using EQCM during potential cycling at relatively higher temperatures,¹¹ and they reported that Pt dissolution is related to two competitive processes: the mechanical detachment of Pt atoms and the electrochemical reduction of Pt oxide. In their study, a lower scan rate than the present study was employed, and they were able to detect the electrochemical dissolution of Pt. However, the potential change was fast during PEFC operation. Thus, we can conclude that the Pt dissolution during PEFC operation is $\text{PtO} + \text{H}^+ + 1/2\text{O}_2 + \text{H}_2\text{O} \rightarrow \text{Pt}(\text{OH})_3^+$ and/or $\text{PtOH} + \text{H}^+ + 3/4\text{O}_2 + 1/2\text{H}_2\text{O} \rightarrow \text{Pt}(\text{OH})_3^+$. Oxygen partial pressure, temperature, and scan rate dependences are now under investigation in detail.

This work was supported by the Fuel Cell Promotion Office of the Agency of Natural Resources and Energy, Ministry of Economy, Trade and Industry (METI) and New Energy,

Industrial Technology Development Organization (NEDO). TK also acknowledges KAKENHI (Grant-in-Aid for Scientific Research (C) (No. 20550009) from Ministry of Education, Culture, Sports, Science and Technology (MEXT) of Japan.

References

- 1 a) *Handbook of Fuel Cells: Fundamentals Technology and Applications*, ed. by W. Vielstich, A. Lamm, H. A. Gasteiger, Wiley, New York, **2004**. b) R. Adzic, in *Electrocatalysis*, ed. by J. Lipkowski, P. N. Ross, VCH Publishers, New York, **1998**, Chap. 5, p. 197. c) S. Gottesfeld, T. A. Zawodzinski, in *Advances in Electrochemical Science and Engineering*, ed. by R. C. Alkire, H. Gerischer, D. M. Kolb, C. W. Tobias, Wiley VCH, Weinham, **1997**, Vol. 5, p. 195. doi:10.1002/9783527616794.ch4.
- 2 a) N. M. Marković, T. J. Schmidt, V. Stamenković, P. N. Ross, *Fuel Cells* **2001**, *1*, 105. b) N. M. Marković, P. N. Ross, *Electrochim. Acta* **2000**, *45*, 4101.
- 3 V. Komanicky, K. C. Chang, A. Menzel, N. M. Markovic, H. You, X. Wang, D. Myers, *J. Electrochem. Soc.* **2006**, *153*, B446.
- 4 a) N. M. Marković, P. N. Ross, Jr., *Surf. Sci. Rep.* **2002**, *45*, 117. b) T. J. Schmidt, V. Stamenkovic, M. Arenz, N. M. Markovic, P. N. Ross, Jr., *Electrochim. Acta* **2002**, *47*, 3765.
- 5 a) Q. Xu, E. Kreidler, D. O. Wipf, T. He, *J. Electrochem. Soc.* **2008**, *155*, B228. b) Q. Xu, T. He, D. O. Wipf, *Langmuir* **2007**, *23*, 9098.
- 6 S. Mitsushima, S. Kawahara, K. Ota, N. Kamiya, *J. Electrochem. Soc.* **2007**, *154*, B153.
- 7 a) A. P. Yadav, A. Nishikata, T. Tsuru, *Electrochim. Acta* **2007**, *52*, 7444. b) Y. Sugawara, A. P. Yadav, A. Nishikata, T. Tsuru, *Electrochemistry* **2007**, *75*, 359.
- 8 a) S. Kawahara, S. Mitsushima, K. Ota, N. Kamiya, *ECS Trans.* **2006**, *3*, 625. b) K. Ota, S. Nishigori, N. Kamiya, *J. Electroanal. Chem. Interfacial Electrochem.* **1988**, *257*, 205.
- 9 K. Kinoshita, J. T. Lundquist, P. Stonehart, *J. Electroanal. Chem. Interfacial Electrochem.* **1973**, *48*, 157.
- 10 a) D. A. J. Rand, R. Woods, *J. Electroanal. Chem. Interfacial Electrochem.* **1972**, *35*, 209. b) D. C. Johnson, D. T. Napp, S. Bruckenstein, *Electrochim. Acta* **1970**, *15*, 1493. c) S. W. Feldberg, C. G. Enke, C. E. Bricker, *J. Electrochem. Soc.* **1963**, *110*, 826. d) H. A. Laitinen, C. G. Enke, *J. Electrochem. Soc.* **1960**, *107*, 773.
- 11 G. Inzelt, B. Berkes, A. Kriston, *Electrochim. Acta* **2010**, *55*, 4742.
- 12 S. Mitsushima, Y. Koizumi, S. Uzuka, K. Ota, *Electrochim. Acta* **2008**, *54*, 455.
- 13 H. Yoshida, T. Kinumoto, Y. Iriyama, Y. Uchimoto, Z. Ogumi, *ECS Trans.* **2007**, *11*, 1321.
- 14 a) A. V. Virkar, Y. Zhou, *J. Electrochem. Soc.* **2007**, *154*, B540. b) Y. Shao-Horn, P. J. Ferreira, G. J. la O', D. Morgan, H. A. Gasteiger, R. Makharia, *ECS Trans.* **2006**, *1*, 185. c) P. J. Ferreira, G. J. la O', Y. Shao-Horn, D. Morgan, R. Makharia, S. Kocha, H. A. Gasteiger, *J. Electrochem. Soc.* **2005**, *152*, A2256.
- 15 A. Taniguchi, T. Akita, K. Yasuda, Y. Miyazaki, *J. Power Sources* **2004**, *130*, 42.
- 16 R. Mohtadi, W.-k. Lee, J. W. Van Zee, *J. Power Sources* **2004**, *138*, 216.
- 17 M. S. Wilson, F. H. Garzon, K. E. Sickafus, S. Gottesfeld, *J. Electrochem. Soc.* **1993**, *140*, 2872.
- 18 a) M. Łukaszewski, A. Czerwiński, *J. Alloys Compd.* **2009**, *473*, 220. b) M. Łukaszewski, A. Czerwiński, *J. Electroanal. Chem.* **2006**, *589*, 38.
- 19 S. Chen, S. Wu, J. Zheng, Z. Li, *J. Electroanal. Chem.* **2009**, *628*, 55.
- 20 H. R. Colón-Mercado, B. N. Popov, *J. Power Sources* **2006**, *155*, 253.
- 21 G.-S. Park, C. Pak, Y.-S. Chung, J.-R. Kim, W. S. Jeon, Y.-H. Lee, K. Kim, H. Chang, D. Seung, *J. Power Sources* **2008**, *176*, 484.
- 22 R. M. Darling, J. P. Meyers, *J. Electrochem. Soc.* **2003**, *150*, A1523.
- 23 a) M. Watanabe, H. Uchida, M. Miura, N. Ikeda, *J. Electroanal. Chem.* **1995**, *384*, 191. b) S. Ye, T. Haba, Y. Sato, K. Shimazu, K. Uosaki, *Phys. Chem. Chem. Phys.* **1999**, *1*, 3653.
- 24 G. Sauerbrey, *Z. Phys. A* **1959**, *155*, 206.